

Title	Improved performances of wideband MEMS electromagnetic vibration energy harvesters using patterned micro-magnet arrays
Authors	Paul, Kankana;Mallick, Dhiman;Roy, Saibal
Publication date	2019-12
Original Citation	Paul, K., Mallick, D. and Roy, S. [2019] 'Improved performances of wideband MEMS electromagnetic vibration energy harvesters using patterned micro-magnet arrays', 19th International Conference on Micro and Nanotechnology for Power Generation and Energy Conversion Applications, PowerMEMS 2019, Krakow, Poland, 2-6 December, 82063206255 (6pp). doi: 10.1109/PowerMEMS49317.2019.82063206255
Type of publication	Conference item
Link to publisher's version	10.1109/PowerMEMS49317.2019.82063206255
Rights	© 2019, IEEE. Personal use of this material is permitted. Permission from IEEE must be obtained for all other uses, in any current or future media, including reprinting/republishing this material for advertising or promotional purposes, creating new collective works, for resale or redistribution to servers or lists, or reuse of any copyrighted component of this work in other works.
Download date	2023-05-05 11:43:04
Item downloaded from	http://hdl.handle.net/10468/10374

Improved Performances of Wideband MEMS Electromagnetic Vibration Energy Harvesters using Patterned Micro-magnet Arrays

Kankana Paul¹, Dhiman Mallick², Saibal Roy^{1,3}

¹*Micro-Nano-Systems Centre, Tyndall National Institute, Cork, T12 R5CP Ireland*

²*Department of Electrical Engineering, IIT Delhi, New Delhi 110016, India*

³*Department of Physics, University College Cork, Cork, T12 YN60 Ireland*

Abstract

The ubiquitous ambient vibrational energy is a potential candidate for solving the pertinent issue of perpetual powering of the numerous deployed wireless sensor nodes. The major roadblock in the materialization of a fully integrated high-efficiency electromagnetic vibration energy harvester is the lack of CMOS compatible magnetic materials and its integration. This work demonstrates the unique advantage of employing high performance stripe patterned array of magnets instead of conventional thin film of magnets which enhances the electromagnetic coupling factor to 53.03 mWb/m by maximizing the magnetic flux gradient within a small footprint and in a precise location. Further, it explores the benefits of employing compact in-plane moving nonlinear MEMS spring architecture, which till date is relatively unreported, that enhances the bandwidth of operation 3 times as compared with its linear counterpart at the cost of reduced peak load power. This detailed study provides a design guideline and opens up the scope for further design optimization for improving overall performance of MEMS Electromagnetic Vibration Energy Harvesters (EM-VEH).

Introduction

Exponential growth of the 'IoT' market is aiding the materialization of 'Smart City', however finding a perpetual powering solution for numerous deployed wireless sensor nodes as a replacement of environment-unfriendly and energy limited batteries are considered as the major roadblock in its implementation. Harvesting energy from omnipresent ambient vibrations has captivated significant research attention over the past decade as a potential solution. The macro-scale electromagnetic transducer [1, 2] outperforms the other conventional harvesters in converting the available vibrations into usable electrical energy, but the lack of matured technology for the fabrication of miniaturized and integrated CMOS-compatible permanent hard-magnets [3] is one of the pertinent issue in implementation of highly efficient MEMS scale electromagnetic vibration energy harvesters. On the other hand, the extensive development in the high performance permanent magnetic materials has enabled it to be employed as a key feature in the plethora of conventional and hitherto unexplored applications including electromagnetic sensors and actuators [4, 5], high density data storage [6, 7] and microfluidics [8].

The spatial tunability of the magnetic fields produced by micropatterned magnets not only offers a high field gradient of 10^6 T/m order [9], but also overcomes the adverse effect of shape dependent 'Demagnetizing field' which is of particular interest in the field of miniaturized EM transducers [10]. However, it requires elegant design strategies to fully exploit this advantage and provide a firm road map to amenable batch fabrication methodologies of such MEMS transducers. Most of the reported MEMS VEHs propose and demonstrate different shapes of microcoils e.g. rectangular, serpentine [11, 12] etc. However, the obtained output power is as low as hundreds of picowatts to few nanowatts owing to the low-efficiency micro-magnets. The optimal coil-magnet interaction can enhance the EM coupling and hence the overall output performance of such MEMS transducers. Though different fabrication techniques such as electrodeposition, sputtering, dry-packing, screen-printing etc. has been explored and employed by a wide range of research community to fabricate CMOS compatible micro magnets [13, 14], however the impact of the distribution of the elements in the micromagnet array on the device performance has drawn very little attention.

This paper gives an insight into the manipulation of complex magnetic field patterns produced by arrays of micropatterned magnets through detailed finite element analysis and provides a design guideline for the optimization of the micromagnets that will systematically enhance the magnetic flux density which in turn would maximize electromagnetic coupling and hence the output power from the electromagnetic vibration energy harvesters (EMVEH's). Firstly, the effectiveness of using array of

stripe patterned magnets instead of a thin film to address the detrimental effect of ‘demagnetizing field’ in novel and compact MEMS EM-VEH system has been explained. Suitable spring architecture has been designed that will facilitate in-plane vibration demonstrating linear and nonlinear characteristics and the output performance of the harvesters are compared on the basis of obtainable peak load power and operable bandwidth highlighting the trade-off between the two which can be addressed with further design optimization.

Design and Finite Element Analysis

The practical implementation of a fully integrated MEMS EM-VEH is heavily restrained not only by the paucity of the CMOS compatible high energy product permanent hard magnets but also by the detrimental effect of shape dependent ‘Demagnetizing field (H_d)’ [15] on the uniformly magnetized thin films. The demagnetizing field and the associated energy product of the magnetic material are expressed as-

$$H_d = -N_d \cdot M$$

$$(BH) = \mu_0 N_d (1 - N_d) M_s^2$$

Where, N_d is the demagnetizing factor that depends on the shape of the magnetic sample ($N_d = 1$ or 0 for samples with out-of-plane or in-plane anisotropy respectively), M_s is the saturation magnetization of the sample and (BH) is the energy product. This counteractive demagnetizing field (H_d) arises from the generation of free magnetic poles near the edges and tends to demagnetize the magnet in a direction opposite to the direction of magnetization which altogether reduces the effective magnetic flux density and the energy product of the magnetic material. Owing to this, the stray magnetic field from a uniformly magnetized thin film emerges mostly from the edges, making the rest of the material incapable of contributing towards the overall magnetic performance of the material. In this predicament replacing the thin film of magnet by optimized pattern of micro-magnet array to intensify the magnetic flux density by creating more magnetic element edges in a precise location has become an attractive solution [16] in implementing a strategically integrated MEMS EM-VEH (Fig.1). However, disparity of this comparison lies in the mismatch of magnetic volume. So in this work, the height of the elements in the array is adjusted to keep the total magnetic volume same as that of a thin film of certain thickness.

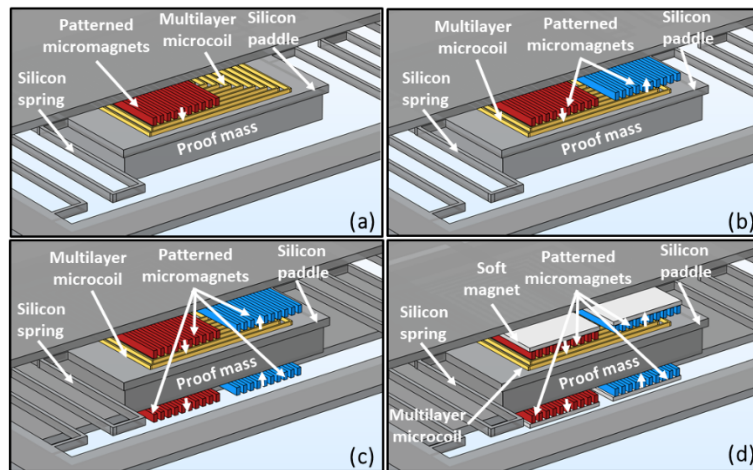


Fig.1. Proposed topologies for the MEMS EM-VEH (a) first topology, (b) second topology, (c) third topology, (d) fourth topology

Four different novel device topologies have been conceived as shown in Fig.1 which consists in-plane moving MEMS-scale silicon springs that holds the rectangular shaped double layer copper micro coils (144 coil turns and 190Ω coil resistance), and a separate substrate containing the pattern of micromagnets, which is flip-chip bonded with the silicon spring layer. In the first topology the magnets are only on one side of the coil, which aids in the generation of higher magnetic flux gradient and hence induced voltage as the coil with the spring move on external vibration from a region of intense magnetic

flux to a region of diminished magnetic flux. The second topology consists of another array of patterned magnet but with an opposite polarization as compared to the adjacent patterns. This enhances the magnetic flux gradient, which is taken a step forward in the third topology by creating an assembly of four array of oppositely polarized magnets such that it forms a closed loop of magnet flux around the micro coil as another layer of magnet is bonded at the bottom of the coil. To further enhance the densification of magnetic flux precisely around the coil, soft magnetic layer is incorporated on the top and bottom layer of the magnets that helps in guiding the magnetic flux lines by minimizing the loss of magnetic field.

The electromagnetic interaction between the square, rectangular shaped coils and micromagnets has been studied employing Ansoft Maxwell simulation tool. In order to generate substantial magnetic stray field, it is possible to geometrically manipulate the micromagnet shapes that will generate maximum magnetic element edges, however keeping in mind the fabrication complexity it is reasonable to consider only simpler geometrical shapes. Owing to the longer edges which are also parallel to the coil tracks, the optimized long-stripe pattern magnet offers substantially enhanced stray fields for relatively thin assembly of magnets (typically below $100\mu\text{m}$ which can be practically achieved employing conventional electrodeposition technique), that in turn also intensifies the magnet-coil interaction [17]. In this study, thin film of magnet (out-of-plane uniform magnetization, Coercivity 0.33T , Retentivity 0.4T) of dimension $1650\mu\text{m} \times 550\mu\text{m} \times 50\mu\text{m}$ is replaced by array of long-stripe patterned magnets each having dimension $1650\mu\text{m} \times 50\mu\text{m} \times 91.67\mu\text{m}$, where the volume of magnetic material lost in the interspacing between the elements is compensated by the height of the stripe magnets in the array.

Here two different spring topologies (Fig.2) have been considered, one resonant type while the other spring demonstrates nonlinear restoring force due to the stretching induced nonlinearity incorporated in it by design. Both of the spring are designed for in-plane motion which on external excitation facilitates more efficient electromagnetic interaction between the coil tracks and the magnet edges as compared with the out-of-plane counterpart [11]. The linear spring architecture comprises of a central moving paddle ($3\text{mm} \times 3\text{mm}$) that holds the proof mass of thickness $350\mu\text{m}$, this is connected to the fixed outer frame through a pair of meandered springs having length 1.9mm and $50\mu\text{m}$ wide.

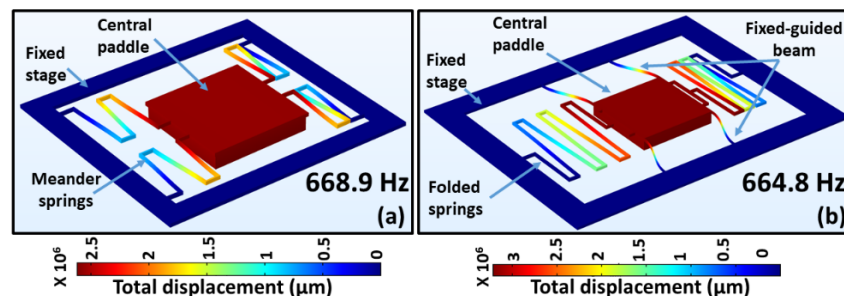


Fig.2. Fundamental modes of oscillation of the designed MEMS spring structures (a)linear and (b)nonlinear

Owing to the scaling, the natural frequency of oscillation of the typical MEMS structure are quite high, to address this issue thicker proof mass (Silicon) is considered in these spring structures to bring the resonant frequency down ($<1000\text{Hz}$) where substantial amount of vibrational energy is distributed. Structural mechanics component of COMSOL Multiphysics has been used as the Finite Element Analysis tool to find the natural frequency, modes of oscillation and the variation of the restoring force with the displacement of the MEMS spring structures. The eigen-frequencies of the first few modes of the designed linear structure are at 668.9Hz , 802.48Hz and 1157.4Hz which corresponds to the in-plane, out-of-plane and tilt motion of the spring. Over the past decade, inclusion of nonlinearity in a wide range of mechanical energy scavengers through geometrical manipulation of the vibrating structures has drawn significant research interest [18-20] as it offers ease in fabrication as well as opens up the scope for study of the complex dynamics of structures. Stretching based nonlinearity has been involved in the systems by means of designing fixed-guided beams, conventionally in the out-of-plane moving structures which at high amplitude of excitation exhibits nonlinear restoring force.

However, the possibility of including such spring-hardening based nonlinearity in MEMS EM-VEH exhibiting in-plane vibration has been unexplored. This work presents additionally a nonlinear MEMS

spring demonstrating in-plane vibration with the help of two set of springs, meandered spring to facilitate in-plane motion and thin clamped-guided spring which is responsible for the inclusion of cubic nonlinearity into such an EM-VEH system. The central paddle, proof mass and thickness of the spring are kept same as that of the linear spring, the thin and short beams attached between the central paddle and the fixed frame experiences stretching as mass on external agitation vibrates in the horizontal direction. The first few modes of vibration are at 664.8Hz, 1774.4Hz and 1921.4Hz, among which the first mode correlates with the in-plane motion. The linear and nonlinear spring stiffness coefficient obtained from the in-plane motion of the nonlinear structure are 480.1 N/m and 1.34×10^{11} N/m³ respectively and the stiffness coefficient of the linear structure is 380.6 N/m.

Table 1. Value of the EM coupling obtained from FEM analysis with different topologies of EM-VEH		
Topology	EM coupling with Square coil (mWb/m)	EM coupling with Rectangular coil (mWb/m)
First (with thin film)	0.88	4.60
First (with stripe pattern)	2.40	10.18
Second (with stripe pattern)	6.79	18.73
Third (with stripe pattern)	16.21	39.40
Fourth (with thin film)	15.28	32.13
Fourth (with stripe pattern and 5µm soft magnet)	21.29	37.78
Fourth (with stripe pattern and 20µm soft magnet)	32.60	53.03

Results and Discussions

The extractable average electrical power over a period of oscillation from the electromagnetic vibration energy harvesters across a suitable load resistance can be expressed as –

$$P_L = \frac{1}{T} \int_0^T \frac{\gamma^2 R_L}{(R_C + R_L)^2} \left(\frac{dz}{dt} \right)^2 dt$$

Where, R_C and R_L are the coil and the load resistance respectively, $\left(\frac{dz}{dt} \right)$ is the velocity of the harvester movement, γ is the electromagnetic coupling factor $\left(= N \cdot \frac{d\phi}{dz} \right)$ between the coil with N turns that experiences a gradient of magnetic flux linkage $\frac{d\phi}{dz}$. Therefore, enhancing the effective interaction between the coil and the magnets could directly result in improved output power performance of the harvester unit.

To investigate the effect of patterned array of magnets on this interaction, two different coil topologies have been used, a conventional square shaped and a rectangular shaped microcoil for the finite element analysis with the four conceived topologies as described earlier. The increased number of magnet element edges in the stripe patterned micromagnets rendering localized and more intense magnetic stray field results in an improved electromagnetic coupling factor of 2.4 mWb/m as compared with 0.88 mWb/m for a thin film of equal volume used in the first topology (Table 1). Further a noticeable improvement could be observed by introducing rectangular coil instead of square coil which yields 10.18 mWb/m coupling factor with the patterned micromagnets and this increment could be attributed to the effective interaction of the long parallel edges of the stripe patterns with each turns of the rectangular coil during the vibration of the magnets, which could not be facilitated by the square coils due to its shape. In the second topology inclusion of the oppositely polarized array of stripe micromagnets intensifies the magnetic flux gradient around which the coil moves engendering the electromagnetic coupling of 18.73 mWb/m, which boosts to more than double the value in the third topology as the same set of oppositely polarized magnet array is placed at the bottom of coil that

strengthens the closed path of magnetic flux. In order to minimize the loss of magnetic field lines from these magnets, in the fourth topology a layer of soft magnet ($5\text{ }\mu\text{m}$ thick and $20\text{ }\mu\text{m}$ thick) is added as indicated in Fig.3 to guide and exacerbate the magnetic field lines. Irrespective of the coil shape used, this envisaged topology leads to a dramatic improvement in electromagnetic coupling to 53.03 mWb/m with rectangular microcoil and 32.60 mWb/m with square coil when a $20\text{ }\mu\text{m}$ thick soft magnet layer is added to the system at the cost of incorporated fabrication complexities. This analysis reveals the efficacy of integrating patterned array of magnets in the MEMS VEH or other Magnetic-MEMS applications instead of thin films, which potentially helps to overcome the degradation of overall performance due to the demagnetizing field.

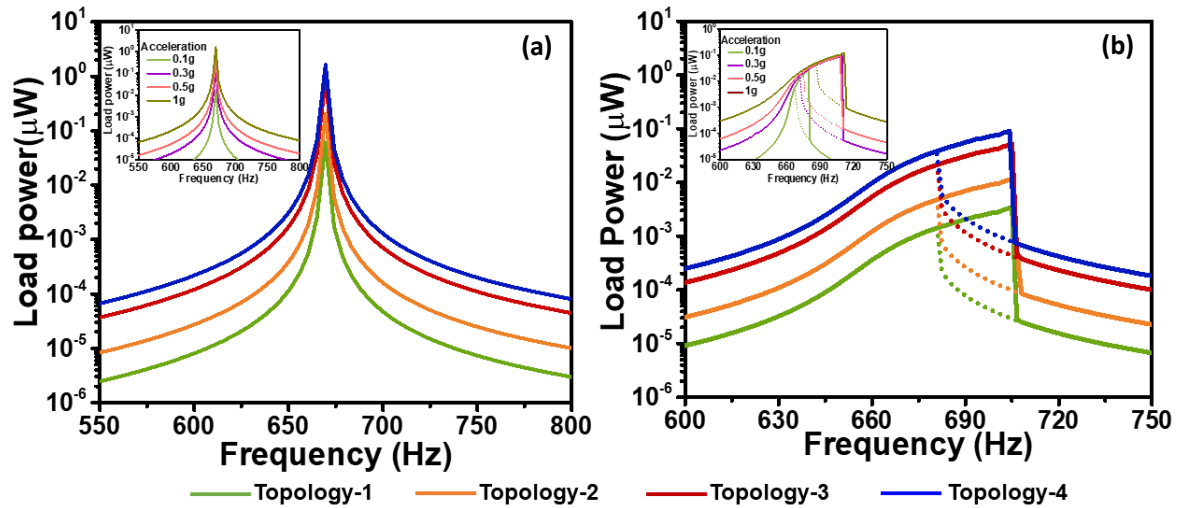


Fig.3. load power response of the (a) linear and the (b) nonlinear vibration energy harvester for different topologies at fixed amplitude of vibration 1g. The inset shows the load power response of the harvester units at different amplitude of external excitation.

To evaluate the overall performance of the energy harvester, and the impact of the improved electromagnetic interaction on the output of the device, variation of the power across the load resistance (190Ω) is studied as the frequency of operation is swept both in the forward and in reverse direction keeping the amplitude of vibration fixed at 1g (Fig.3). The load power for the linear spring rises sharply around the resonant frequency 668.9 Hz to $0.06\mu\text{W}$, $0.20\mu\text{W}$, $0.92\mu\text{W}$, $1.67\mu\text{W}$ for the first, second, third and fourth topology respectively with the half-power bandwidth 8.43 Hz . Despite of the consistent improvement in the output power, these typical resonant transducers suffer from reduced off-resonance efficiency, which makes it unsuitable for efficient vibrational energy scavenging as the energy is distributed over a wide range of frequency components. To address this issue, spring hardening based nonlinearity is used in the second MEMS spring architecture which demonstrates wideband characteristics enabling it to harvest usable electrical energy from a wider range of frequencies. The half-power bandwidth of the energy harvester increases to 24.2 Hz , which is approximately 3 times higher than the linear counterpart at the cost of the reduced peak load power of $0.003\mu\text{W}$, $0.01\mu\text{W}$, $0.05\mu\text{W}$, $0.12\mu\text{W}$ for the first, second, third and fourth topology respectively. The bandwidth enhancement arising from the deliberate inclusion of the nonlinearity into the system can be further increased using stiffer spring or by exciting the system with higher amplitude of vibration (as indicated in inset of Fig.3(b)). This study brings out a critical trade-off between the obtainable load power and the operable bandwidth of the MEMS vibration energy harvesters which can be addressed by optimizing the wide range of tunable parameters e.g. proof mass, degree of nonlinearity, mechanical and electrical damping etc. to implement a high performance fully integrated MEMS EM-VEH.

Conclusion

Abundant availability of ambient vibrations has made it a significant renewable energy source that can be harnessed to solve the powering issues of Wireless Sensor Nodes for 'IoT'. One of the major

impediments in miniaturizing high-efficiency macro-scale Electromagnetic Vibrational Energy Harvester (EM-VEH) prototypes into the MEMS scale is the lack of matured technology for the CMOS compatible integration of magnets and the adverse effect of scaling on the permanent hard magnets. The present work demonstrates a systematic approach to overcome these constraints by integrating optimized patterned micromagnets in the energy harvester unit with the motivation of intensifying the magnetic field distribution at precise location which on interaction with high density microcoil generates larger electrical power of $1.67\mu\text{W}$ with a linear MEMS spring and $0.12\mu\text{W}$ with an in-plane moving nonlinear MEMS spring across suitable load owing to the enhanced electromagnetic coupling of 53.03 mWb/m which proves the efficacy of the proposed design strategy.

Acknowledgements

This work is financially supported by a research grant from Science Foundation Ireland (SFI) and is co-funded under the European Regional Development Fund Grant Number 13/RC/2077. This is also part funded by the EU-H-2020 project 'Enables', Project ID: 730957.

References

- [1] P. Constantinou and S. Roy, "A 3D printed electromagnetic nonlinear vibration energy harvester," *Smart Materials and Structures*, vol. 25, no. 9, p. 095053, 2016/08/24 2016.
- [2] D. Mallick, A. Amann, and S. Roy, "Surfing the High Energy Output Branch of Nonlinear Energy Harvesters," *Physical Review Letters*, vol. 117, no. 19, p. 197701, 11/04/ 2016.
- [3] D. P. Arnold, "Review of Microscale Magnetic Power Generation," *IEEE Transactions on Magnetics*, vol. 43, no. 11, pp. 3940-3951, 2007.
- [4] M. Han, Q. Yuan, X. Sun, and H. Zhang, "Design and Fabrication of Integrated Magnetic MEMS Energy Harvester for Low Frequency Applications," *Journal of Microelectromechanical Systems*, vol. 23, no. 1, pp. 204-212, 2014.
- [5] D. Niarchos, "Magnetic MEMS: key issues and some applications," *Sensors and Actuators A: Physical*, vol. 109, no. 1, pp. 166-173, 2003/12/01/ 2003.
- [6] S. N. Piramanayagam, "Perpendicular recording media for hard disk drives," *Journal of Applied Physics*, vol. 102, no. 1, p. 011301, 2007/07/01 2007.
- [7] T. Dutta, S. N. Piramanayagam, T. H. Ru, M. S. M. Saifullah, C. S. Bhatia, and H. Yang, "Exchange coupled CoPt/FePtC media for heat assisted magnetic recording," *Applied Physics Letters*, vol. 112, no. 14, p. 142411, 2018/04/02 2018.
- [8] H. Li, T. J. Flynn, J. C. Nation, J. Kershaw, L. Scott Stephens, and C. A. Trinkle, "Photopatternable NdFeB polymer micromagnets for microfluidics and microrobotics applications," *Journal of Micromechanics and Microengineering*, vol. 23, no. 6, p. 065002, 2013/04/22 2013.
- [9] D. L. Roy *et al.*, "Fabrication and characterization of polymer membranes with integrated arrays of high performance micro-magnets," *Materials Today Communications*, vol. 6, pp. 50-55, 2016/03/01/ 2016.
- [10] Y. Tanaka *et al.*, "Design Optimization of Electromagnetic MEMS Energy Harvester with Serpentine Coil," in *2013 IEEE International Conference on Green Computing and Communications and IEEE Internet of Things and IEEE Cyber, Physical and Social Computing*, 2013, pp. 1656-1658.
- [11] M. Han, Z. Li, X. Sun, and H. Zhang, "Analysis of an in-plane electromagnetic energy harvester with integrated magnet array," *Sensors and Actuators A: Physical*, vol. 219, pp. 38-46, 2014/11/01/ 2014.
- [12] Y. Tanaka *et al.*, "Electromagnetic Energy Harvester by Using NdFeB Sputtered on High Aspect Ratio Si Structure," *Journal of Physics: Conference Series*, vol. 476, p. 012095, 2013/12/04 2013.
- [13] N. Jackson, F. J. Pedrosa, A. Bollero, A. Mathewson, and O. Z. Olszewski, "Integration of Thick-Film Permanent Magnets for MEMS Applications," *Journal of Microelectromechanical Systems*, vol. 25, no. 4, pp. 716-724, 2016.
- [14] Y. Jiang *et al.*, "Fabrication of NdFeB microstructures using a silicon molding technique for NdFeB/Ta multilayered films and NdFeB magnetic powder," *Journal of Magnetism and Magnetic Materials*, vol. 323, no. 21, pp. 2696-2700, 2011/11/01/ 2011.
- [15] J. M. D. Coey, "Hard Magnetic Materials: A Perspective," *IEEE Transactions on Magnetics*, vol. 47, no. 12, pp. 4671-4681, 2011.
- [16] D. Mallick, K. Paul, T. Maity, and S. Roy, "Magnetic performances and switching behavior of Co-rich CoPtP micro-magnets for applications in magnetic MEMS," *Journal of Applied Physics*, vol. 125, no. 2, p. 023902, 2019/01/14 2019.
- [17] S. Roy, D. Mallick, and K. Paul, "MEMS-Based Vibrational Energy Harvesting and Conversion Employing Micro-/Nano-Magnetics," *IEEE Transactions on Magnetics*, vol. 55, no. 7, pp. 1-15, 2019.
- [18] D. Mallick, A. Amann, and S. Roy, "A nonlinear stretching based electromagnetic energy harvester on FR4 for wideband operation," *Smart Materials and Structures*, vol. 24, no. 1, p. 015013, 2014/11/27 2014.
- [19] B. Marinkovic and H. Koser, "Smart Sand—A Wide Bandwidth Vibration Energy Harvesting Platform," *Applied Physics Letters - APPL PHYS LETT*, vol. 94, 03/09 2009.
- [20] P. Podder, D. Mallick, A. Amann, and S. Roy, "Influence of combined fundamental potentials in a nonlinear vibration energy harvester," *Scientific Reports*, Article vol. 6, p. 37292, 11/22/online 2016.

Corresponding author: Saibal Roy, Tyndall National Institute, University College Cork,
Address: Lee Maltings, Dyke parade, Cork, Ireland, T12 R5CP, Phone: (0) 21234 6331,
Email: saibal.roy@tyndall.ie